EFFECT OF CAVITY DIAMETER AND PRESSURE ON POOL BOILING BUBBLE DYNAMICS

Jionghui Liu[1*], Daniel Orejon[1], Jonathan G. Terry[2], Anthony J. Walton[2], Camelia Dunare[2], Khellil Sefiane[1]

[1]School of Engineering, Institude for Multiscale Thermofluids, University of Edinburgh, Edinburgh, EH9 3FD, United Kingdom
[2]School of Engineering, Institude for Micro and Nano Systems, University of Edinburgh, Edinburgh, EH9 3FF, United Kingdom

ABSTRACT

Bubble behaviour, as nucleation, growth, coalescence, and departure, during the boiling process is an important phenomenon affecting heat transfer and heat removal performance. Observing the bubble behaviour is a crucial method to understanding the boiling heat transfer mechanism. This work studies the dynamics of single bubble nucleating and departing from isolated artificial cavities with different diameters on a SiO_2 coated surfaces. The experiments were conducted in FC-72 under saturation pressures varying from 0.75 bar to 1.75 bar. The bubble behaviour during nucleation was investigated using a high-speed camera. During a complete bubble growth period, the FC-72 bubble is spherical. After the initial growth period, its only contact with the boiling surface is by what we have termed the narrow 'vapour bridge'. The size of the contact area is affected by the cavity diameter: a larger bubble departure diameter for a larger cavity mouth. The bubble departure diameter increases from 0.45 mm for a 20 µm cavity diameter to 0.61 mm for a 70 µm cavity diameter. In addition, a higher saturation pressure will generate bubbles with smaller departure diameters: they decreasing from 0.62 mm for 0.75 bar to 0.47 mm for 1.75 bar. The bubble departure diameter does not change significantly with different degree of superheat for similar cavity diameter and saturation pressure. The bubble departure frequency increases linearly with increasing degree of superheat. While pressure has a limiting effect on bubble departure frequency, larger cavity diameter on the other hand leads to lower bubble departure frequency.

1. INTRODUCTION

Nucleation pool boiling plays a crucial role in the thermal management systems such as high-power systems and electrical devices like electric vehicles, photovoltaics, and supercomputers [1]. Unlike single-phase heat transfer, nucleation pool boiling two-phase change can attain higher heat-transfer coefficients with smaller interface temperature increase and more effective area for heat removal due to the high energy transfer resulting from the phase-change process [2].

A great amount of research was focused on the bubble growth and its departure as a convenient and effective method to investigate the performance of the boiling mechanisms. Bosnjaković et al. [3] firstly introduced a model that proposes that the latent heat utilised for the evaporation of the bubble comes from the thin superheated liquid layer surrounding the bubble. Since then, many researchers have aimed to test this theory experimentally and modified bubble growth equations have been proposed [4]. Thereafter Fritz [5] established the static force balance between surface tension and buoyancy forces to predict bubble departure diameter, which influences the boiling process, and several works have improved the theory under different working conditions [6].

With the increasing demand of heat removal ability for high power and electrical devices, smooth surfaces are not enough to achieve a high heat-transfer coefficient. Hence, surfaces with different roughness, wettability, and textures are implemented to achieve higher heat transfer coefficients. One of the most significant challenges is to provide reliable and effective heat removal performance, which has led to a great interest for investigating the enhancement mechanisms owed to the different surface

*Corresponding Author: jionghui.liu@ed.ac.uk

characteristics [7]. It is then clear that bubble behaviour is completely different on structured surfaces when compared to the traditional smooth surfaces. In this case, it is more difficult to understand the heat transfer mechanise due to the intricate bubble behaviour as a consequence of the different surface roughness, wettability, structure, etc. There is still no universally acceptable heat transfer mechanism and theoretical model to predict the heat transfer process on advanced surfaces.

This current work has updated Hutter's [1] experimental rig and investigated bubble growth dynamic behaviour on surfaces with different characteristics, particularly focussing on single bubble behaviour from cavities varying in diameters. The bubble growth and departure performance were analysed and compared for different cavity diameters, superheat degrees and saturation pressures. The findings give support to further works on multiple bubble interactions and on surface characteristic effect on pool boiling heat transfer performance.

2. APPARATUS AND BOILING SURFACE

2.1 Experimental apparatus

The experimental apparatus is illustrated in Figure 1 (a). Pool boiling experiment was performed in a boiling chamber, equipped with four bottom heaters and two surround heating pads to maintain the FC-72 liquid at the saturation temperature. Two T-type thermocouples were used to measure the vapour and liquid temperature from the top and bottom of the boiling chamber respectively, with ± 0.1 K temperature accuracy. A digital pressure gauge with ± 0.1 % accuracy at room temperature measured the pressure of the boiling chamber. The boiling chamber pressure could be controlled from 0.5 bar to 3.0 bar by adjusting the flow rate and temperature of coiling water in the external condenser. The accuracy of the thermal bath temperature control is ± 0.1 K.

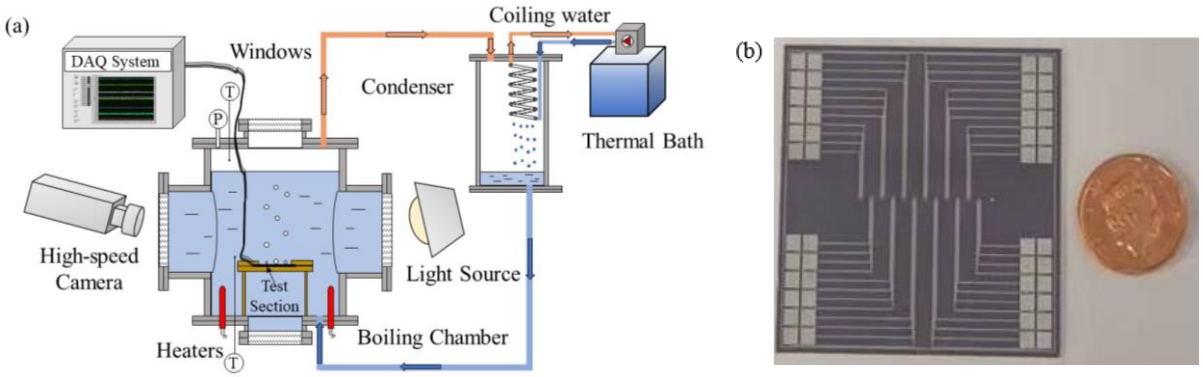

Figure 1: (a) Experimental setup of the boiling chamber and (b) front side of the boiling surface.

The boiling surface is investigated on a PEEK (polyether ether ketone) polymer jig located in the centre of the boiling chamber with spring probes provides an electrical connection. The boiling surface is a 50 × 50 mm^2 silicon substrate with 12 micro-fabricated temperature sensors on the front side as shown in Figure 1 (b) and a micro-fabricated aluminium heater on the backside. A SiO_2 layer as shown in Figure 2 (b) coats the front surface to achieve hydrophilic performance. The distance between each sensor is 2 mm and each sensor has a 0.5 × 0.5 mm^2 area (as shown in Figure 2 (c)) to achieve the average temperature under each bubble. Each sensor has four connections, of which two are used to pass a constant current through the sensor and the remaining two to measure the voltage. The linear relationship between the sensor resistance and the temperature can be used to estimate the surface temperature. The temperature sensors were calibrated before and after experiments with T-type thermocouples with an accuracy of ± 0.1 K between 20 ℃ and 95 ℃. Artificial cavities with different diameters were then etched in the centre of each temperature sensor, as shown in Figure 2 (d). The detailed micro-fabrication process is described in previous work [1].

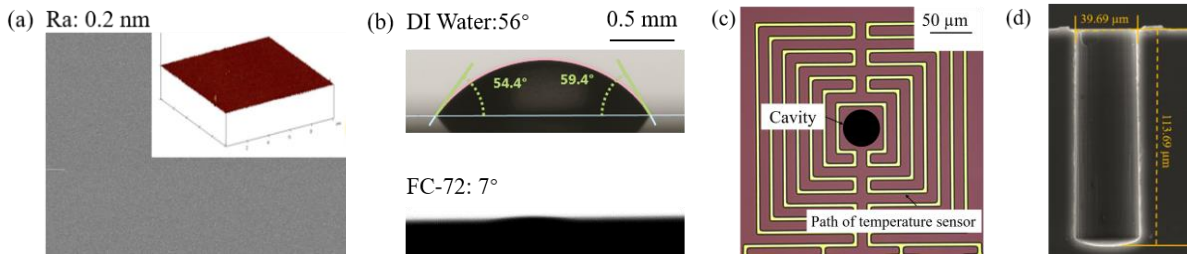

Figure 2: Close-up photograph of (a) SEM and AFM measurement, (b) contact angle for DI water and FC-72, (c) optical image of a micro-sensor and (d) SEM image of an etched cavity.

A high precision multimeter (196 System DMM, Keithley Instruments Inc.) recorded the voltage from the temperature sensor and pressure data from the pressure transducer. A high-speed camera recorded the bubble growth at frames rates from 1000 fps to 15000 fps. A trigger device was used to synchronise the high-speed camera and data acquisition system. The bubble diameter and departure frequency were determined from high-speed videos. For the bubble growth diameter measurements, the measurement error was ± 2 px from image resolution. In addition, the measurement error of the bubble departure frequency was estimated to be ±1 ms. The detailed experimental procedure can be found in previous works [1].

3. RESULTS AND DISCUSSION

3.1 Bubble growth rate

The relevant parameters characteristic of the bubble dynamics (including bubble growth diameter, bubble departure diameter and departure frequency) were determined by image sequences further analysed with ImageJ software. In Figure 3 (a), a sequence of images with 2 ms intervals is shown for an entire bubble growth cycle from a 150 µm deep cavity with a 35 µm diameter at 4.2 K superheat and 1.25 bar saturation pressure. The bubble shape is spherical during growth and departure and only contacts the surface through the 'vapour bridge' that holds the bubble attached to the surface. The schematic diagram of the bubble outline and bubble contact angle (θ) during the whole period is shown in Figure. 3 (b).

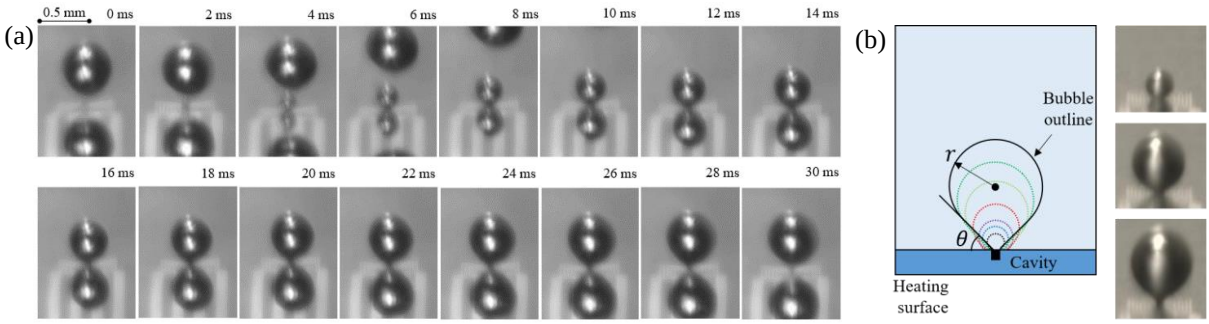

Figure 3: (a) High-speed photos of a bubble growth from a 35 µm diameter cavity at 4.2 K superheat and 1.25 bar saturation pressure and (b) bubble outline for isolate bubble growth.

The bubble growth diameter for different superheat degrees is shown in Figure 4. The diameter of the bubble shows a nearly linear increase during the initial period, i.e., the first milliseconds, with similar growth rates for the various superheat degrees studied. After the initial period, the higher superheat degree could achieve a faster growth rate due to higher input power.

From the image sequences, the bubble growth diameter, base contact area and contact angle can be measured, as shown in Figure 5. The base contact area increases from around 0.04 mm to 0.07 mm during the initial period with 3.9 K superheat degree. The cavity diameter of 0.035 mm, which means that the bubble baseline growth exceeds the cavity mouth dimensions. Meanwhile, the bubble contact angle decreases from 80° to around 40° as shown in Figure 5 (a). This indicates that the bubble

microlayer area increases during the initial period, leading to the linear increase in bubble diameter reported. After the initial period, the contact area reaches the maximum value and then slowly decreases until it approximately reaches the diameter of the cavity mouth. During this growth period, the contact angle remains constant and then quickly increases during departure. During departure, the 'necking' phenomenon appears [8], i.e., the 'vapour bridge' between the bubble and the surface becomes thinner until it breaks at the mid-point. Then the top bubble departs from the surface and a tiny fraction of the bubble vapour remains within and above the cavity. The remaining vapour will then continue to grow creating the next bubble. There is no waiting time between the departure bubble and the new bubble because of the vapour trapped and left within the cavity and above it. The contact area shows a rapid increase and decrease during bubble growth at 7.8 K superheat degree as shown in Figure 5 (b).

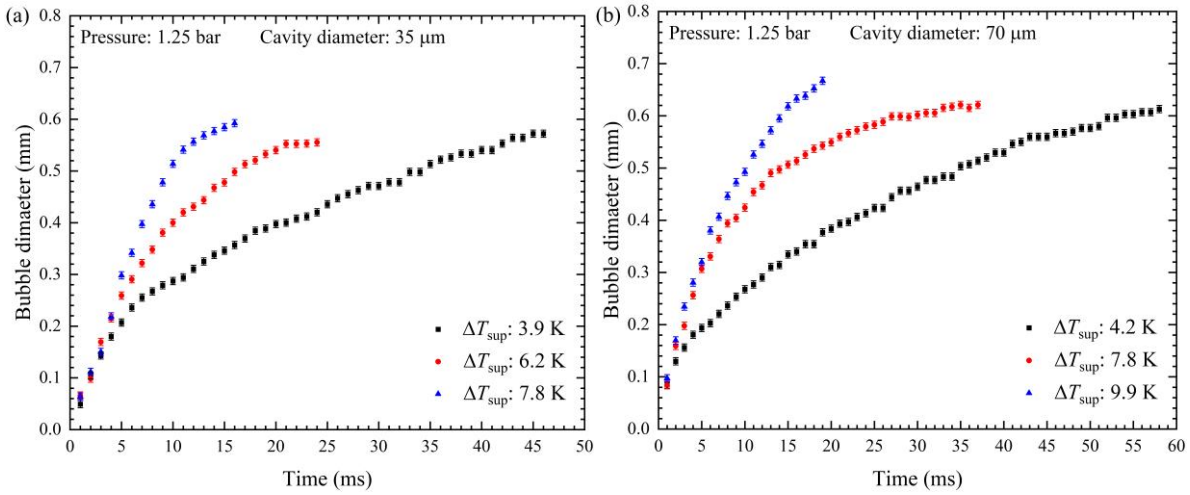

Figure 4. Bubble growth diameter with different superheat degree for (a) 35 μm and (b) 70 μm cavity diameter

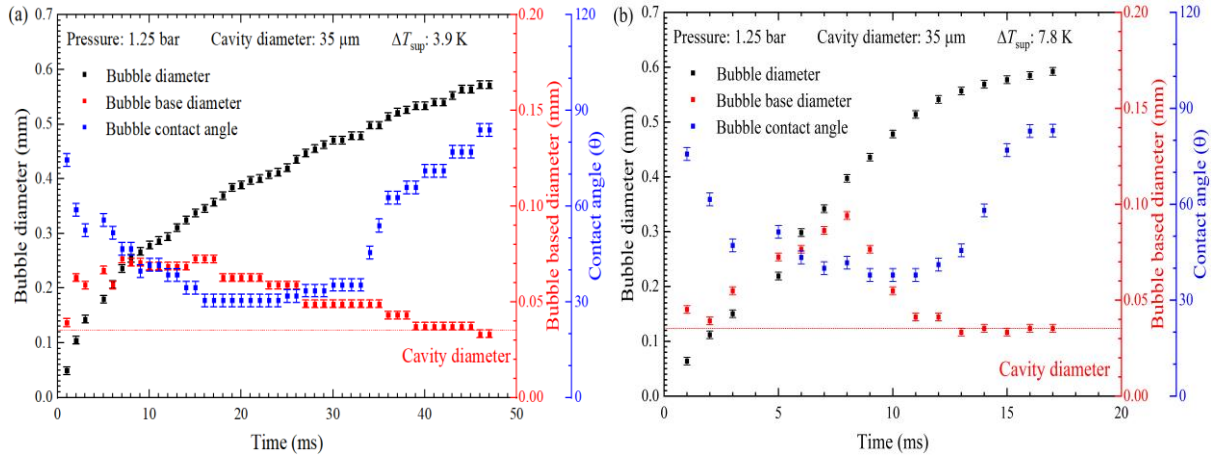

Figure 5. Bubble growth diameter, contact diameter and contact angle with (a) 3.9 K and (b) 7.8 K superheat degree

3.2 Effect of cavity diameter and pressure on bubble growth performance

Figure 6 shows the data obtained of the bubble growth diameter with different cavity diameters and saturation pressures. The measurement error is ± 2 px (about 0.007 mm) from image resolution. The effect of cavity size on bubble growth is not obvious during the initial fast growth period (0 ms to 10 ms). The absolute deviation of bubble diameter for the same growth time is less than 0.05 mm as shown in Figure 6 (a). For bubble growth times after more than 15 ms, the larger the cavity diameter, the larger the bubble's diameter. The bubble departure diameter is 0.45 mm for a 20 μm cavity diameter, 0.55 mm for a 40 μm cavity diameter and 0.61 mm for a 70 μm cavity diameter. The bubble growth diameters are compared for several saturation pressures in Figure 6 (b). The bubble departure diameter shows a decrease for higher system pressures. The average departure diameter ($D_{d,ave.}$) increased about 32 % from 0.47 mm for 1.75 bar to 0.62 mm for 0.75 bar with about 3.9 K superheat degree.

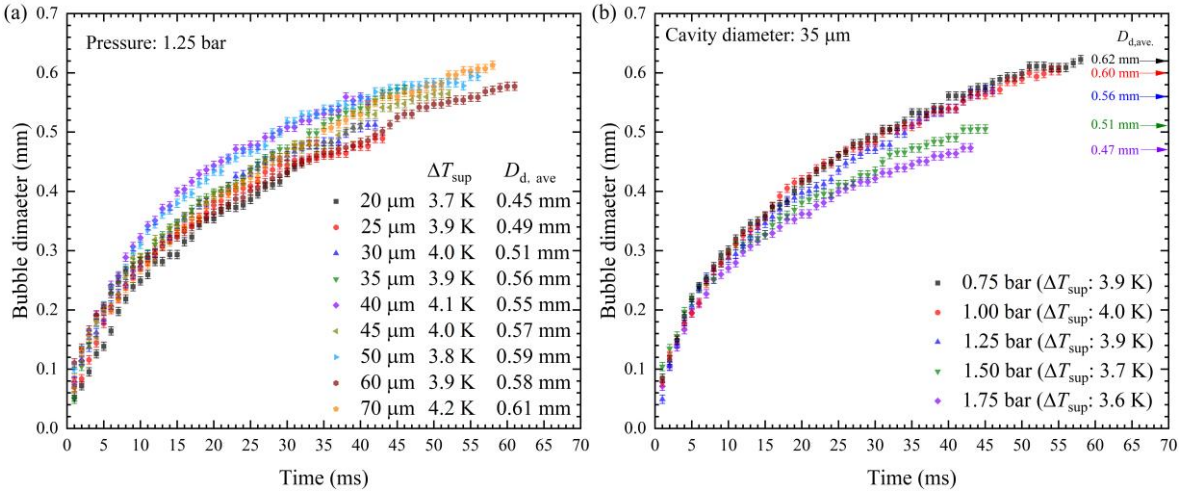

Figure 6: Bubble growth rate with different (a) cavity diameters and (b) saturation pressure.

3.3 Effect of cavity diameter on bubble departure performance

Figure 7 shows the data obtained for the bubble departure diameter and departure frequency with different cavity diameters from three successive bubbles. In Figure 7 (a), the bubble departure diameter is nearly constant with superheat degree increases from 2 K to 8 K. Moreover, with larger cavities the departure diameter shows a clear increase. The average departure diameter is around 0.46 mm for 20 μm cavity diameter and around 0.60 mm for 70 μm cavity diameter. The larger cavity diameter achieves larger contact area between bubble and surface, which in turn leads to larger surface tension forces being needed to overcome the buoyance force. This will delay bubble departure period, resulting in the observation of larger bubble departure diameters. The bubble departure frequency in Figure 7 (b) shows a linear increase with increasing superheat degree. The larger cavity diameter is more likely to result in lower bubble departure frequency at similar superheat degree. It is about 10 Hz for 70 μm cavity diameter with 5 K superheat degree, rising to 40 Hz for 30 μm cavity diameter with similar superheat degree.

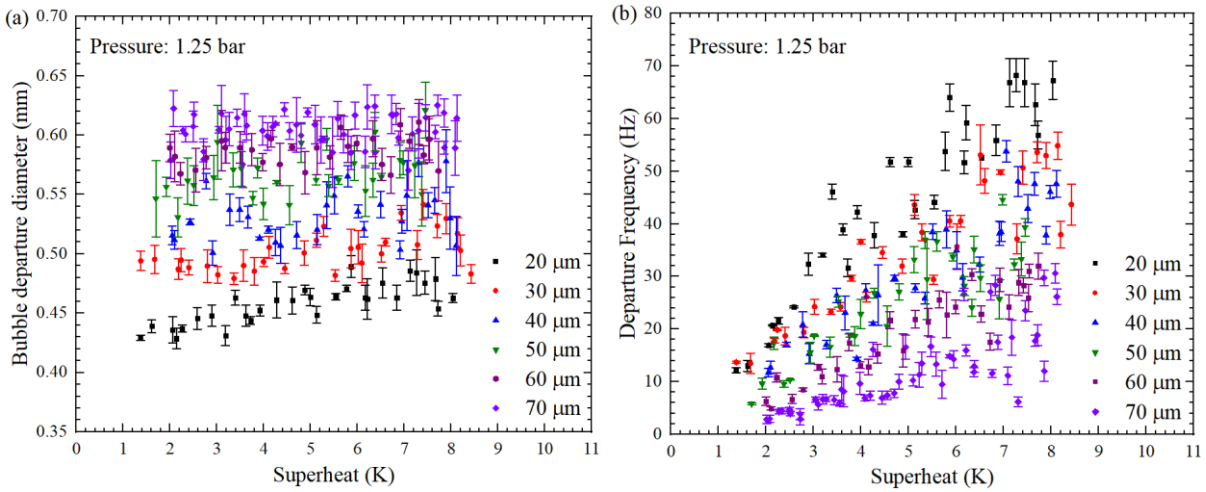

Figure 7: Bubble (a) departure diameter and (b) departure frequency with different cavity diameters.

Figure 8 shows the bubble departure behaviour at different saturation pressure. A smaller bubble departure diameter is obtained for higher pressure as shown in Figure 8 (a). It decreases from around 0.63 mm at 0.75 bar saturation pressure to 0.47 mm at 1.75 bar saturation pressure for the same cavity diameter of 0.04 mm. In addition, the bubble departure diameter has a nearly constant value for different superheat degrees at similar saturation pressure. The bubble departure frequency increases linearly with superheat degree increase for the same cavity diameter of 0.04 mm. The pressure impact on bubble departure frequency is limited as shown in Figure 8 (b).

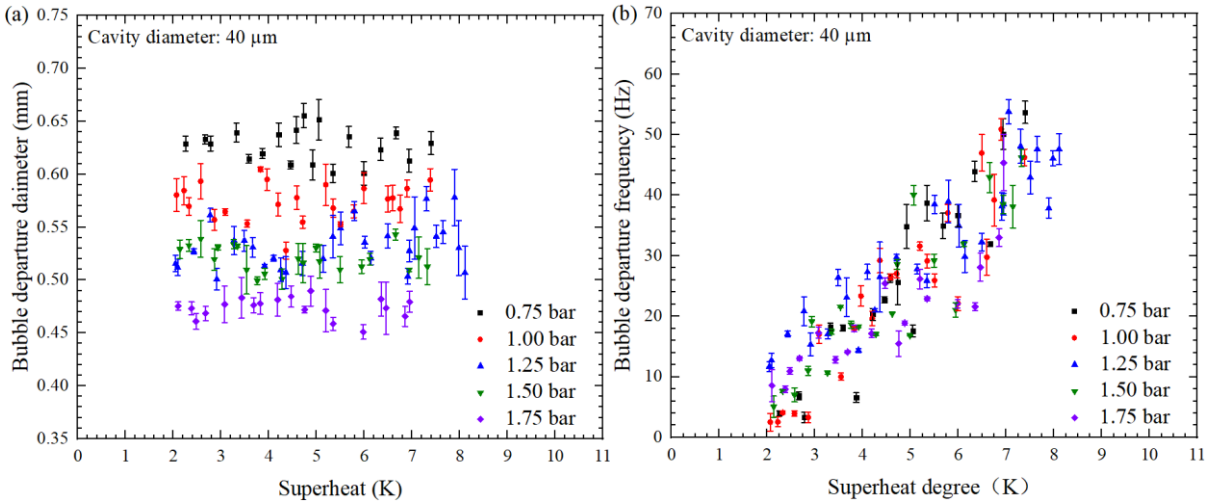

Figure 8: Bubble (a) departure diameter and (b) departure frequency with different saturation pressures.

4. CONCLUSIONS

Pool boiling experiments have been performed using silicon substrate, coated with a hydrophilic layer of SiO_2, to investigate the bubble dynamics resulting from different cavity diameters and saturation pressures. Larger cavity diameters result in larger bubble departure diameters and lower bubble departure frequency. The saturation pressure also affects bubble departure diameter with a 32 % increase measured between 0.75 bar and 1.75 bar. However, saturation pressure has limited impact on bubble departure frequency. In addition, when superheat degree increases from 2 K to 8 K, the bubble departure diameter remains nearly constant for similar cavity diameters and saturation pressures.

ACKNOWLEDGEMENTS

We acknowledge support from EPSRC of the UK (EP/S019588/1). The experimental surfaces were manufactured on silicon wafers at the University of Edinburgh's cleanroom facilities housed in the Scottish Microelectronics Centre.

REFERENCES

[1] Hutter, C., Kenning, D. B. R., Sefiane, K., Karayiannis, T. G., Lin, H., Cummins, G., & Walton, A. J. Experimental pool boiling investigations of FC-72 on silicon with artificial cavities and integrated temperature microsensors [J]. *Experimental Thermal and Fluid Science*, 2010, 34(4): 422-433.

[2] Mudawar I. Assessment of high-heat-flux thermal management schemes [J]. *IEEE transactions on components and packaging technologies*, 2001, 24(2): 122-141.

[3] Bosnjaković F. Verdampfung und Flüssigkeitsüberhitzung [J]. *Technische Mechanik und Thermodynamik*, 1930, 1(10): 358-362.

[4] Zuber N. The dynamics of vapor bubbles in nonuniform temperature fields [J]. *International Journal of Heat and Mass Transfer*, 1961, 2(1-2): 83-98.

[5] Friz W. Maximum volume of vapor bubbles [J]. *Physic. Zeitschz.*, 1935, 36: 379-354.

[6] Zhou J, Xu P, Qi B, et al. Effects of micro-pin-fins on the bubble growth and movement of nucleate pool boiling on vertical surfaces [J]. *International Journal of Thermal Sciences*, 2022, 171: 107186.

[7] Li W, Dai R, Zeng M, et al. Review of two types of surface modification on pool boiling enhancement: passive and active [J]. *Renewable and Sustainable Energy Reviews*, 2020, 130: 109926.

[8] Jo H J, Ahn H S, Kang S H, et al. A study of nucleate boiling heat transfer on hydrophilic, hydrophobic and heterogeneous wetting surfaces [J]. *International Journal of Heat and Mass Transfer*, 2011, 54(25-26): 5643-5652.